The pulsating brain: an interface-coupled fluid-poroelastic model of the cranial cavity

Marius Causemann
Vegard Vinje
Marie E. Rognes
Simula Research Laboratory
Dept. for Scientific Computing and Numerical Analysis

Cardiac pulsations drive oscillatory motion in the cranial cavity

[Nevit Dilmen, NPH patient, Wikimedia Commons, 2010]

The disbalance of arterial inflow and venous outflow drives pressure pulsations and CSF flow

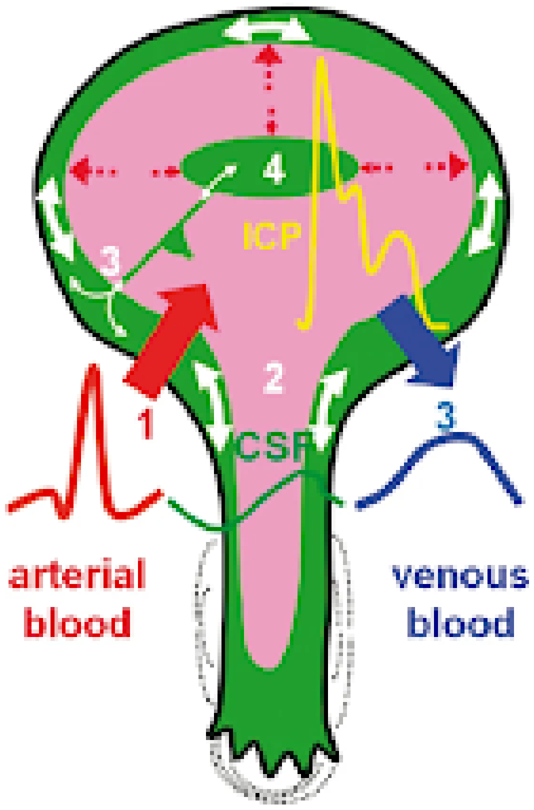

[Balédent, Olivier. "Imaging of the cerebrospinal fluid circulation" *Adult hydrocephalus* (2014)]

A computational framework for intracanial pulsatility

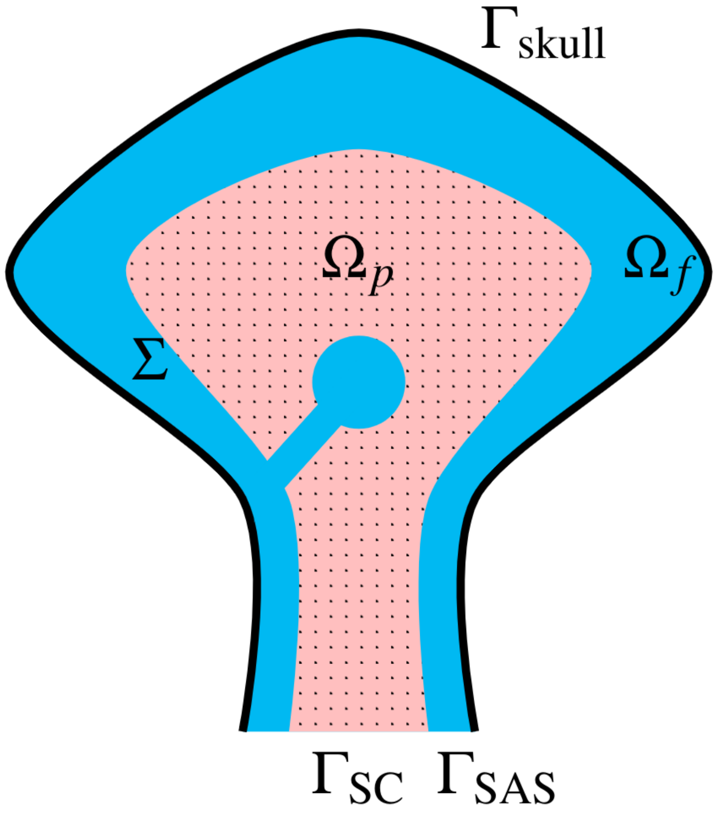

a) Stokes flow - CSF-filled spaces - Ω_f

$$\rho_F \partial_t \mathbf{u} - \text{ div } [2\mu_F \epsilon(\mathbf{u}) - p_F \mathbf{I}] = 0$$
$$\text{div } \mathbf{u} = 0$$

b) Poroelasticity (Biot) - brain tissue - Ω_p

$$-\mathbf{div}[2\mu_S \epsilon(\mathbf{d}) + \lambda \text{ div } \mathbf{d} - \alpha p_p \mathbf{I}] = 0$$
$$c_0 \partial_t p_p - \alpha \partial_t \text{ div } \mathbf{d} + \text{ div } \left(\frac{\kappa}{\mu_F} \nabla p_p \right) = g$$

c) Interface conditions on Σ

The disbalance of arterial inflow and venous outflow drives intracranial pulsatile motion

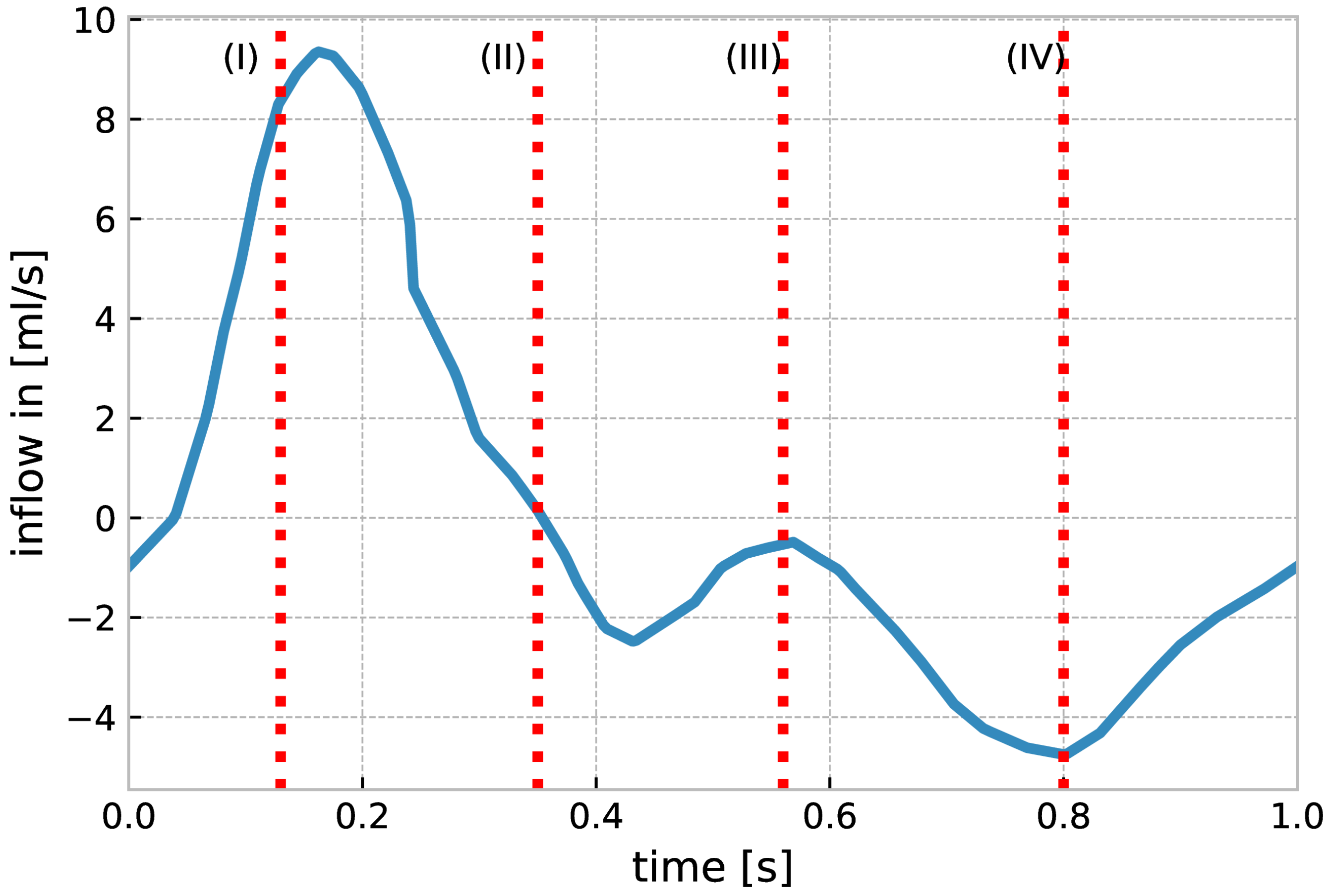

(I) early systole - high net blood inflow

(I) end of net blood inflow

(III) brain equilibrium phase

(IV) high net outflow of blood

varying in time, spatially uniform mass source term g

The model is based on a detailed, MRI-derived geometry

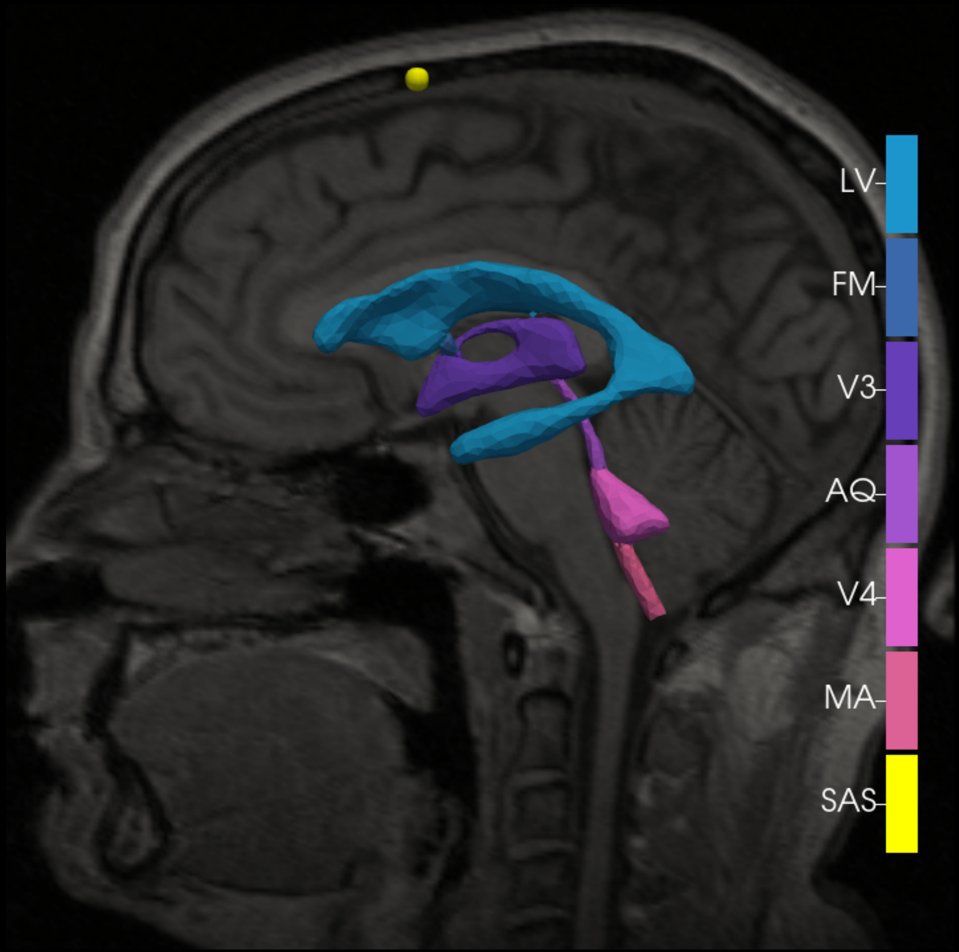

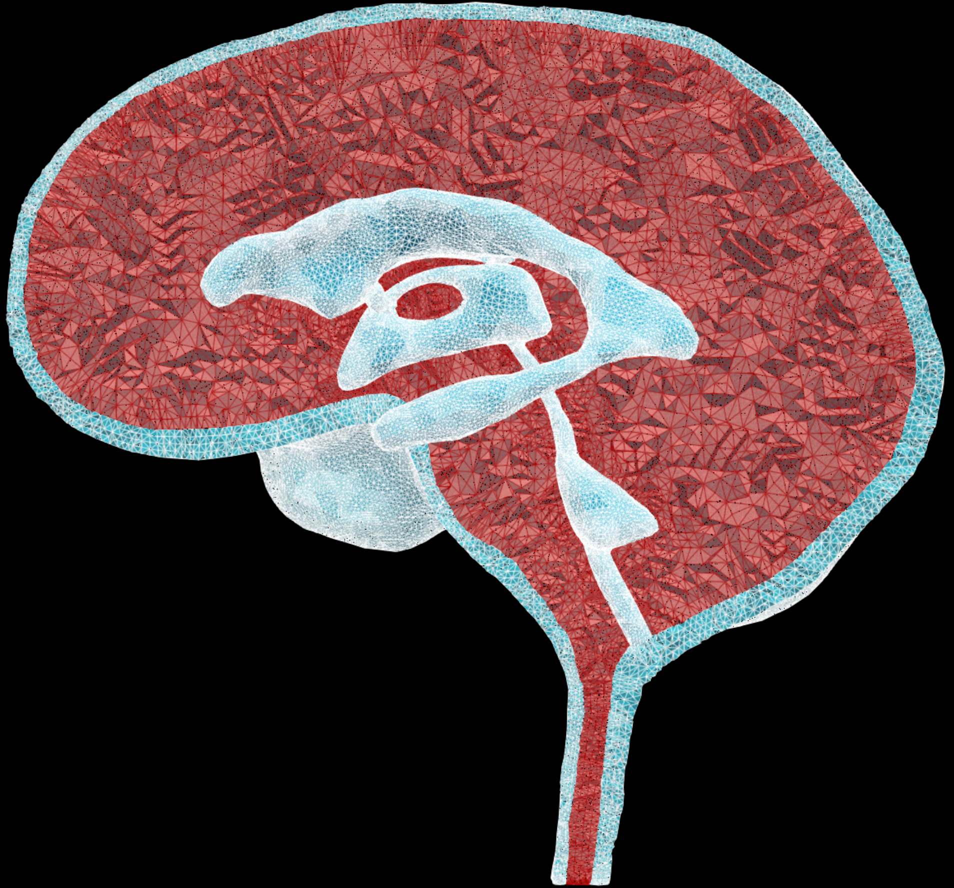

The fluid-poroelastic coupling is based on first principles

Mass conservation on Σ

$$\mathbf{u} \cdot \mathbf{n} = \left(\partial_t \mathbf{d} + \frac{\kappa}{\mu_F} \nabla p_P \right) \cdot \mathbf{n}$$

Momentum conservation on Σ

$$(2\mu_F \epsilon(\mathbf{u}) - p_F \mathbf{I})\, \mathbf{n} = (2\mu_S \epsilon(\mathbf{d}) - \phi \mathbf{I})\, \mathbf{n}$$

Balance of total normal stress on Σ

$$p_p + \mathbf{n} \cdot (2\mu_F \epsilon(\mathbf{u}) - p_F \mathbf{I})\, \mathbf{n} = 0$$

Beavers-Joseph-Saffman condition on Σ

$$-\mathbf{n} \cdot (2\mu_F \epsilon(\mathbf{u}) - p_F \mathbf{I})\, \tau_i = \frac{\gamma \mu_F}{\sqrt{\kappa}} (\mathbf{u} - \partial_t \mathbf{d}) \cdot \tau_i$$

with the tangential vectors $\tau_i, i = 1, 2$

The boundary conditions represent a rigid skull and a compliant spinal compartment

Rigid skull

$$\mathbf{u} = 0 \qquad \text{on } \Gamma_{\text{skull}}$$

Spinal coord

$$\mathbf{d} = 0 \quad \text{and} \quad \frac{\kappa}{\mu_f} \nabla p_p \cdot \mathbf{n} = 0 \qquad \text{on } \Gamma_{\text{SC}}$$

Spinal SAS

$$(2\mu_f \epsilon(\mathbf{u}) - p_f \mathbf{I}) \cdot \mathbf{n} = -\mathbf{n}\, p_0 \cdot 10^{\Delta V_{\text{out}}(t)/\text{PVI}_{\text{SC}}} \ \text{on } \Gamma_{\text{SAS}}$$

$$\text{with } \Delta V_{\text{out}}(t) = \int_0^t \int_{\Gamma_{\text{SAS}}} \mathbf{u} \cdot \mathbf{n} \ \mathrm{d}s \, \mathrm{d}t$$

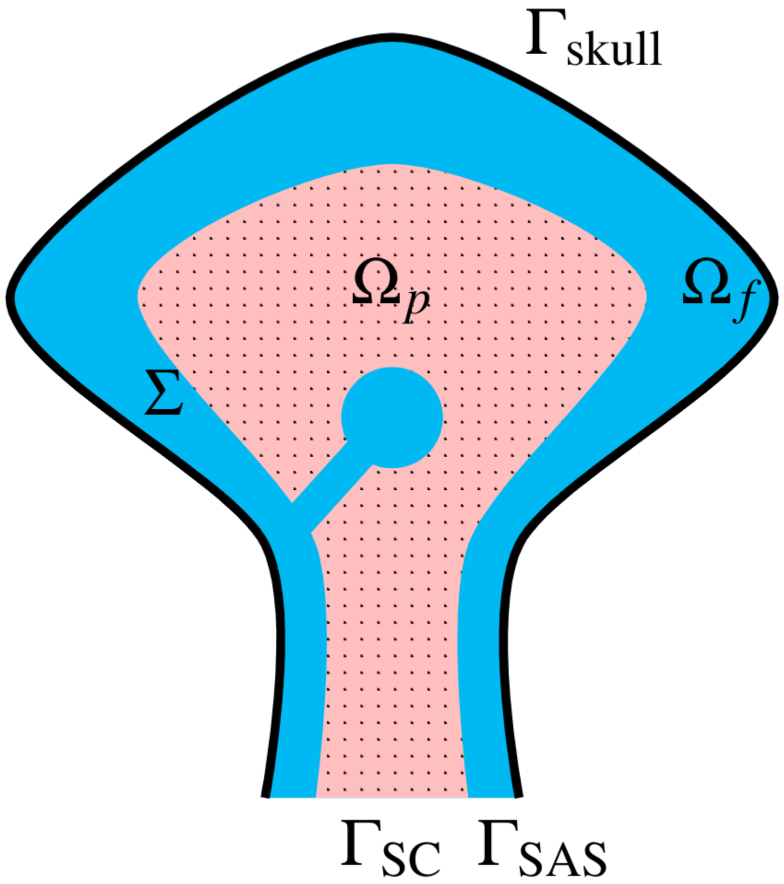

The model is solved using a monolithic finite element approach

- total pressure formulation for Biot
- Taylor-Hood type elements (P2-P1-P2-P1-P1)
- implicit Euler time discretization

Block System

At each time step, find $\mathbf{u}_h^{n+1}, p_{F,h}^{n+1}, \mathbf{d}_h^{n+1}, p_{P,h}^{n+1}$ and ϕ such that

$$\begin{bmatrix} \mathcal{A}^F & (\mathcal{B}_1^F)' & \frac{1}{\Delta t}(\mathcal{B}_3^\Sigma)' & (\mathcal{B}_2^\Sigma)' & 0 \\ \mathcal{B}_1^F & 0 & 0 & 0 & 0 \\ \mathcal{B}_3^\Sigma & 0 & \mathcal{A}_1^P & (\mathcal{B}_4^\Sigma)' & (\mathcal{B}_1^P)' \\ -\mathcal{B}_2^\Sigma & 0 & -\frac{1}{\Delta t}\mathcal{B}_4^\Sigma & \mathcal{A}_2^P & -\frac{1}{\Delta t}(\mathcal{B}_2^P)' \\ 0 & 0 & \mathcal{B}_1^P & \mathcal{B}_2^P & -\mathcal{A}_3^P \end{bmatrix} \begin{bmatrix} \mathbf{u}_\mathrm{h}^{\mathrm{n}+1} \\ p_{F,h}^{n+1} \\ \mathbf{d}_\mathrm{h}^{\mathrm{n}+1} \\ p_{P,h}^{n+1} \\ \phi_h^{n+1} \end{bmatrix} = \begin{bmatrix} \mathcal{F}^{F,n} \\ 0 \\ \mathcal{F}^{P,n} \\ \mathcal{G}^n \\ 0 \end{bmatrix}$$

Implementation

- direct solver (MUMPS)
- implementation based on Fenics & Multiphenics

Variations in the ICP are dominated by their temporal amplitude

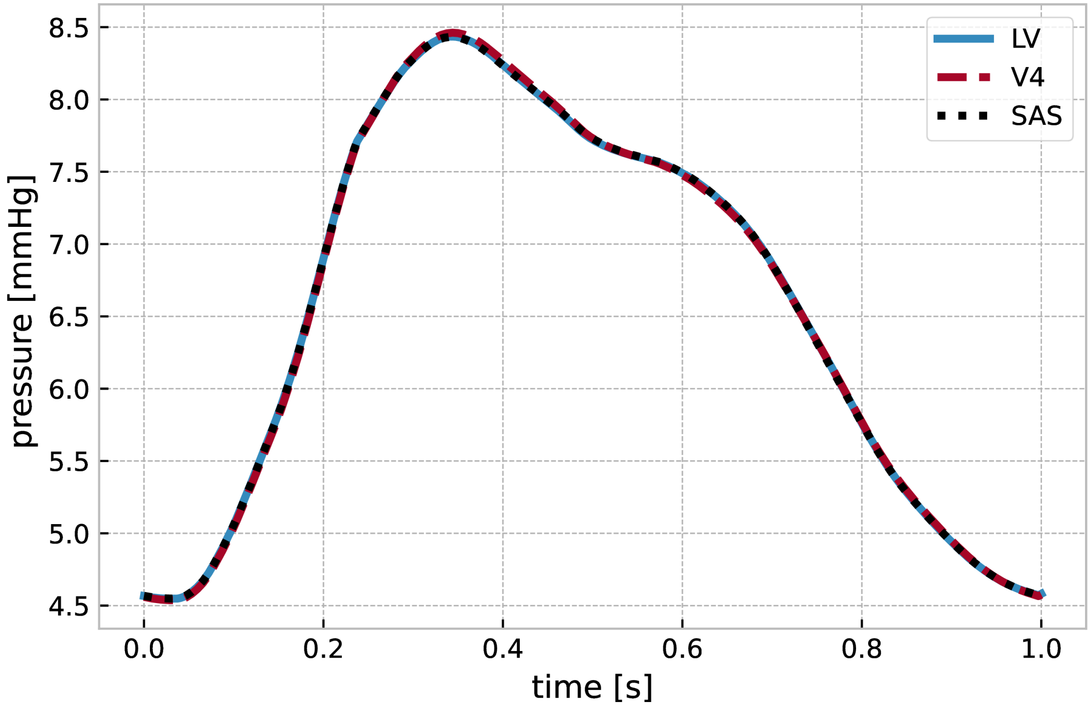

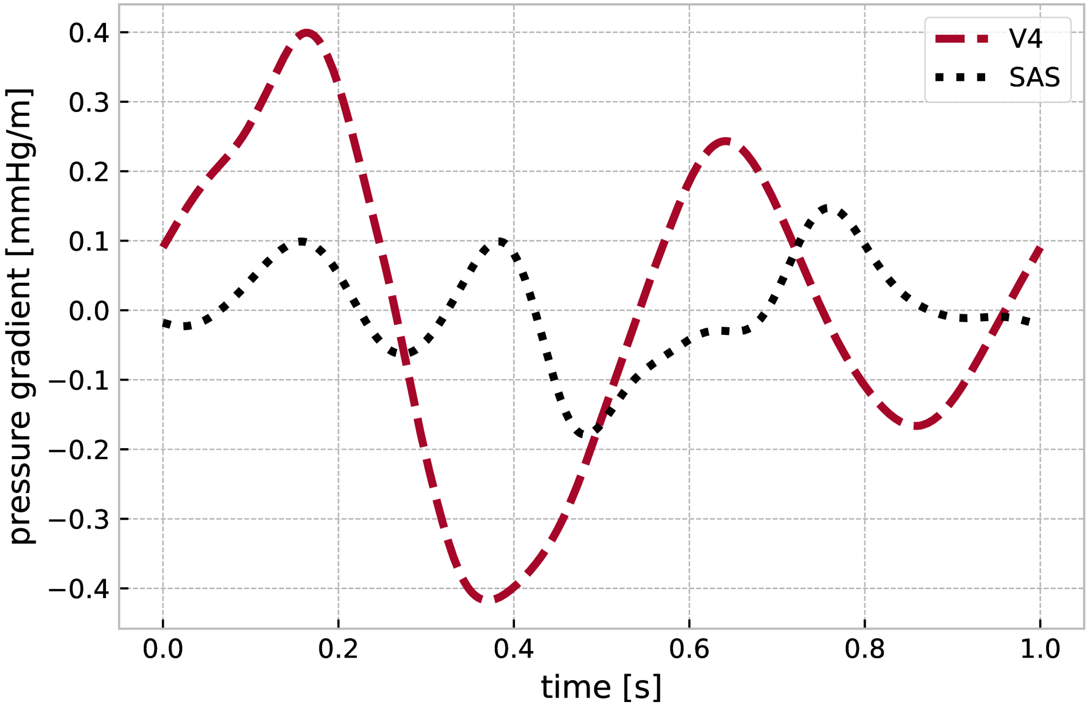

Cardiac pulsations cause substantial pressure variations and complex flow patterns

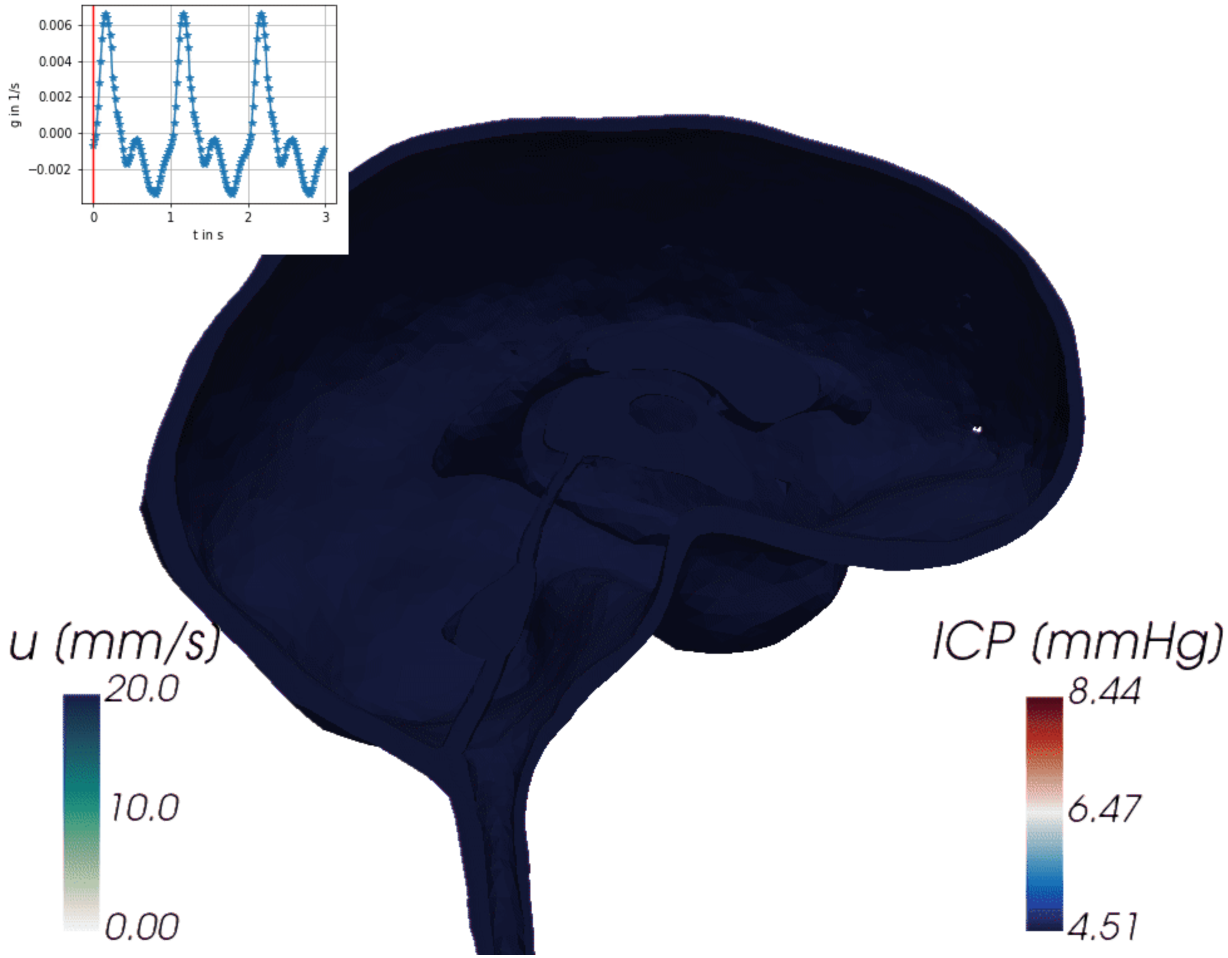

The largest peak flow rates occure into the spinal canal

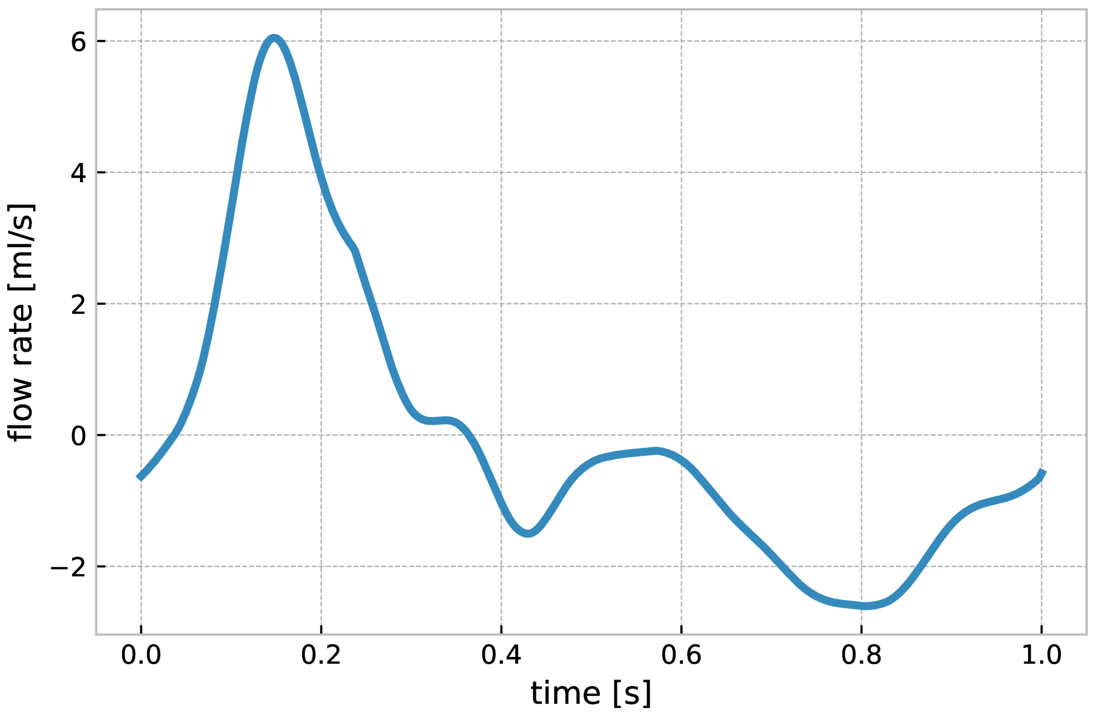

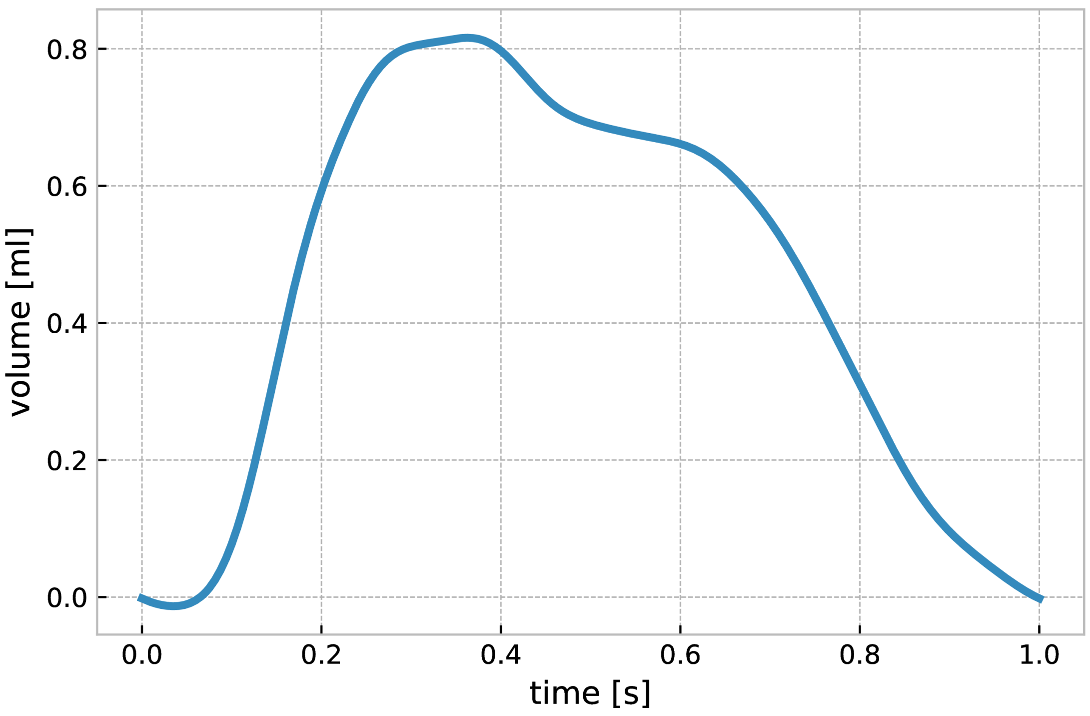

The largest peak flow rates occure into the spinal canal

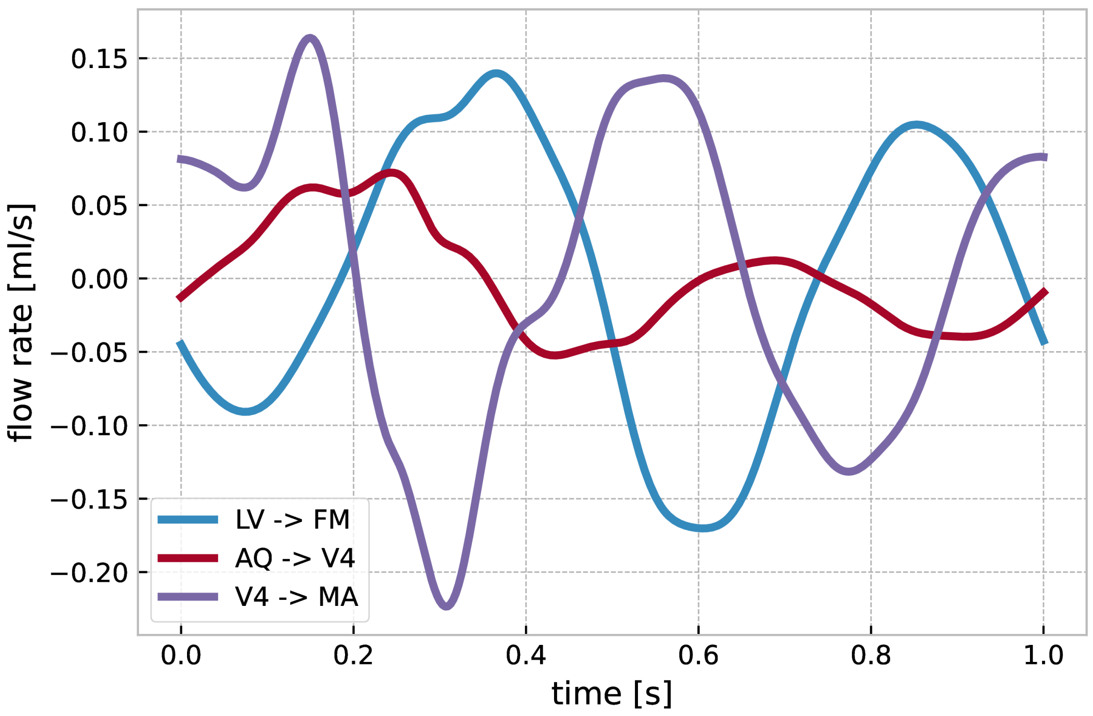

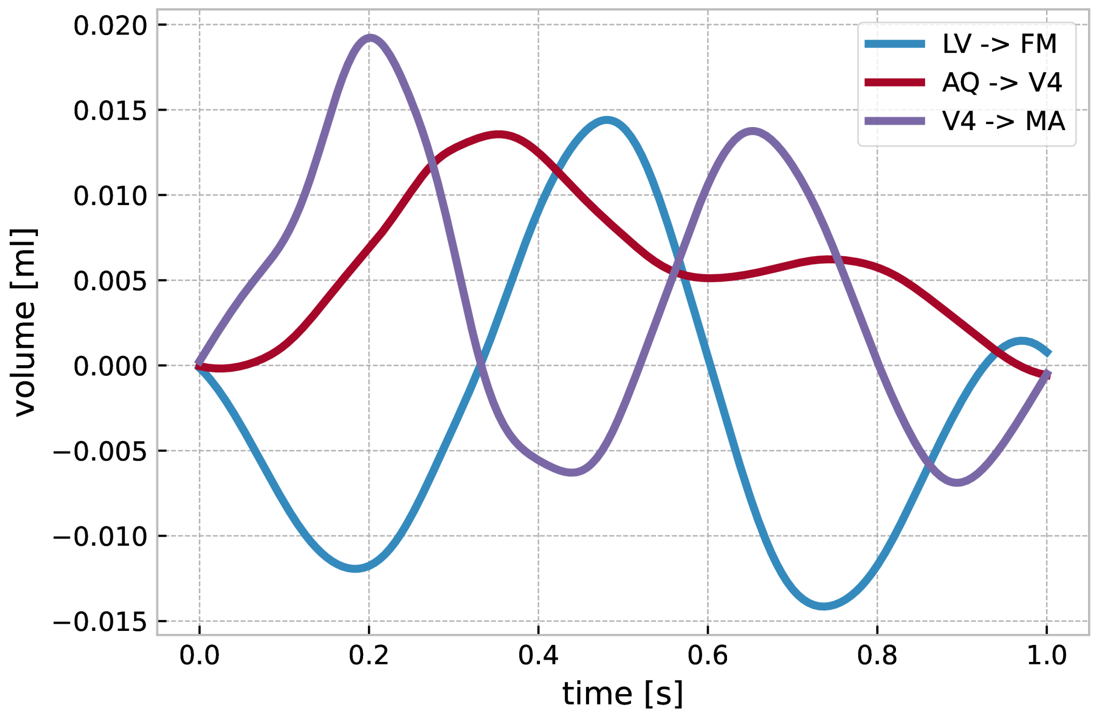

The brain tissue rotates and exhibits a funel-shaped motion at the brain stem

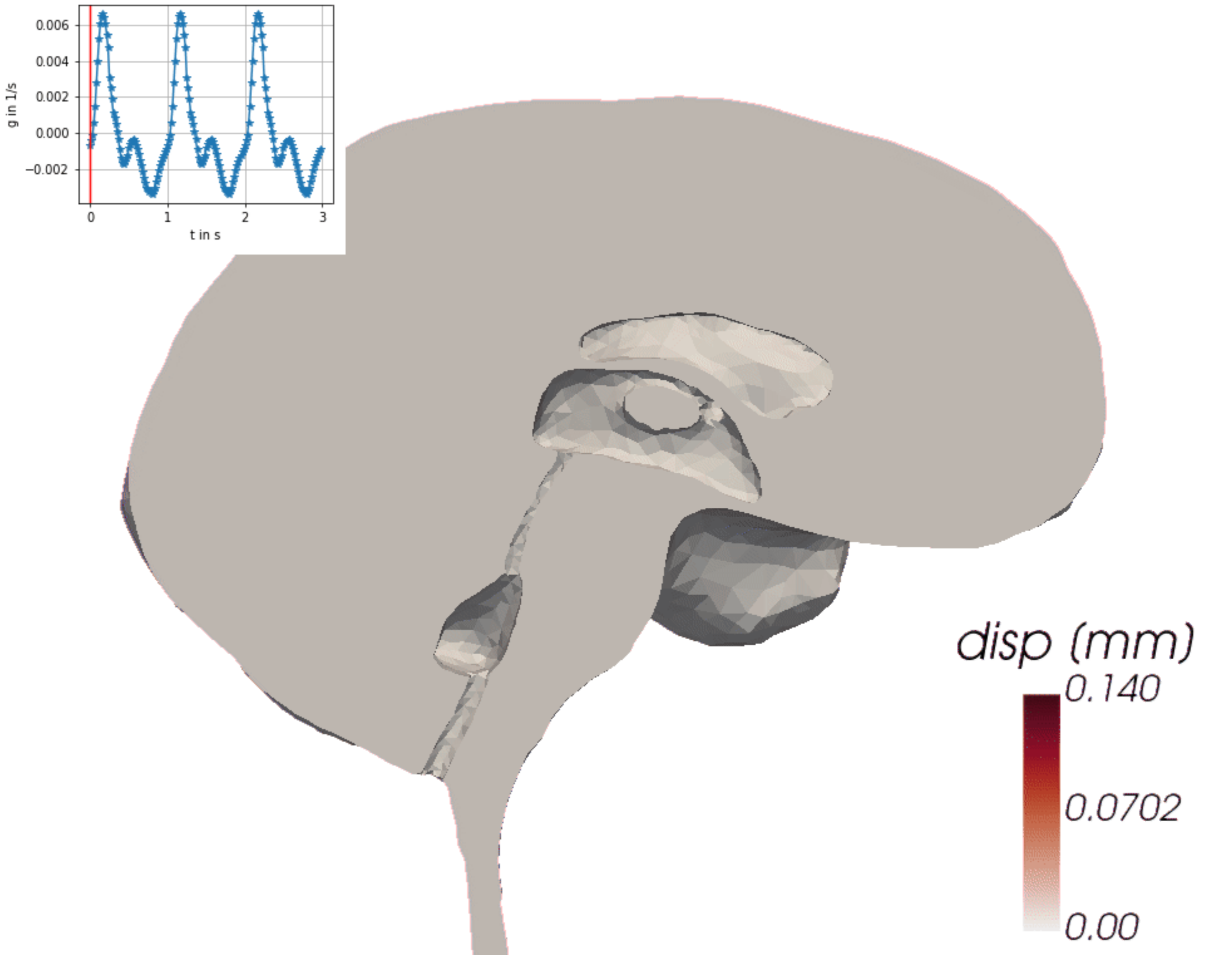

We compute the effect of a selection of parameter deviations

Model	modified parameter	value	interpretation
Standard	-	-	-
A	pressure-volume index	$\mathrm{PVI} = 10\,\mathrm{ml}$	greater spinal compliance
B	Young Modulus	$E = 3000\,\mathrm{Pa}$	stiffer brain parenchyma
C	Poisson ratio	$\nu = 0.4$	greater compressibility of parenchymal tissue
D	storage coefficient	$c = 10^{-5}\mathrm{Pa}^{-1}$	greater cranial compliance

Model variations

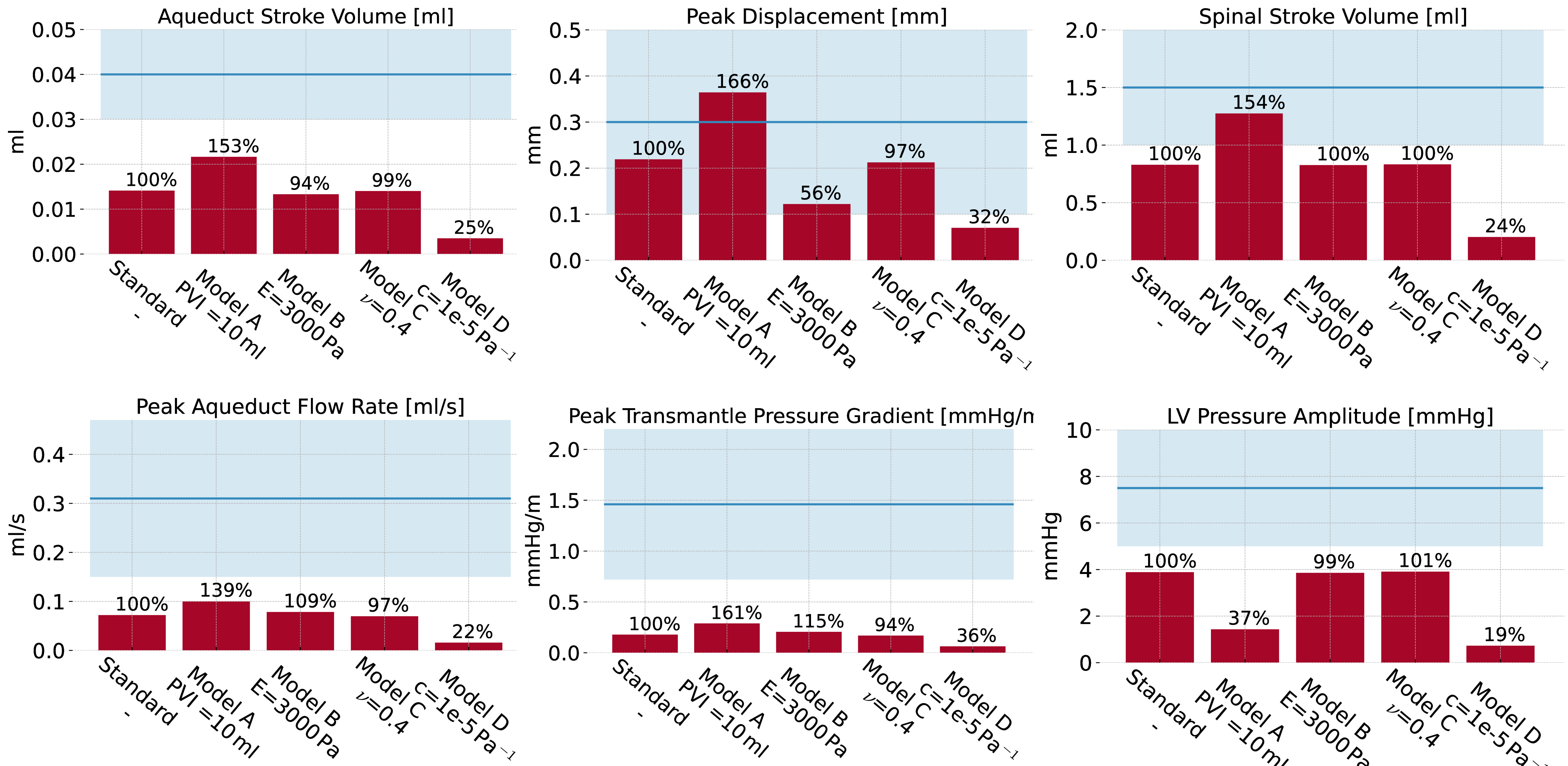

In conclusion, we present a new computational framework of cardiac-induced intracranial motion

our model predicts ICP, CSF flow and tissue displacement with high resolution in space and time

new insights into intracranial pulsatility in health and disease

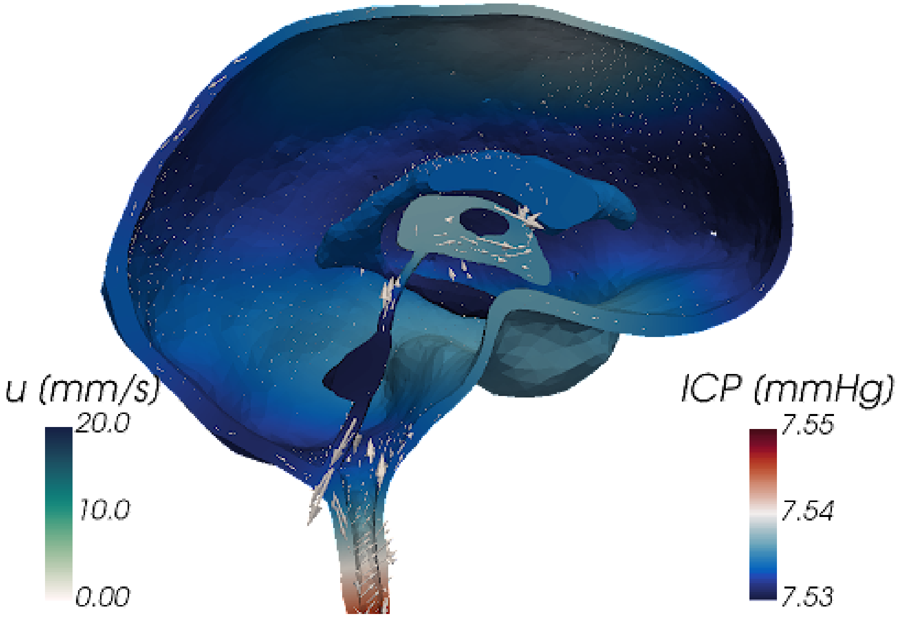

10.1101/2022.05.19.4

bioRxiv
THE PREPRINT SERVER FOR BIOLOGY

simula EMIx

Causemann, M., Vinje, V., & Rognes, M. E. (2022). *Human intracranial pulsatility during the cardiac cycle: a computational modelling framework*, biorxiv